Chemical Engineering Journal 288 (2016) 869–879

Contents lists available at ScienceDirect

Chemical Engineering Journal

journal homepage: www.elsevier.com/locate/cej

Adsorption of vanillin and syringaldehyde onto a macroporous polymeric resin

Maria Inês F. Mota, Paula C. Rodrigues Pinto, José Miguel Loureiro, Alírio E. Rodrigues *

LSRE – Laboratory of Separation and Reaction Engineering – Associate Laboratory LSRE/LCM, Faculdade de Engenharia, Universidade do Porto, Rua Dr. Roberto Frias, 4200-465 Porto, Portugal

HIGHLIGHTS

- SP700 is a nonpolar resin suitable for vanillin (V) and syringaldehyde (S) adsorption.
- Batch experiments were successfully fitted with Langmuir and Freundlich models.
- Maximum adsorption capacities obtained: 0.663 (V) and 0.707 (S) g $g^{-1}_{dry\_resin}$.
- SP700 showed 46% more capacity for V than reported in literature for other resins.
- Fixed bed experiments were described with the axially dispersed plug flow model.

GRAPHICAL ABSTRACT

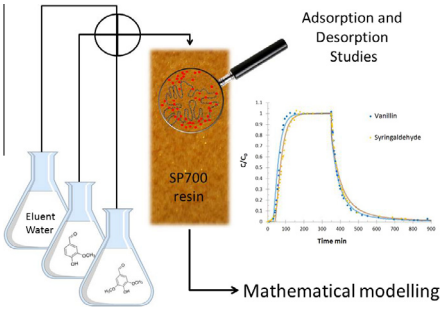

ARTICLE INFO

Article history:
Received 13 October 2015
Received in revised form 11 December 2015
Accepted 12 December 2015
Available online 17 December 2015

Keywords:
Vanillin
Syringaldehyde
Adsorption
Nonpolar resin
Breakthrough

ABSTRACT

Pulp and paper mill and biorefinery side-streams are rich in lignin which can be partially converted to vanillin and syringaldehyde through an oxidation process. These value-added compounds can be recovered with an integrated separation process encompassing an adsorption step. In this work the potential of a macroporous polymeric resin, Sepabeads SP700, was assessed.

The resin was characterized regarding particle size, solid density, apparent density and particle porosity by means of laser dispersion, helium pycnometry and mercury intrusion porosimetry, respectively. Values within the ranges given by supplier were achieved: solid density, apparent density, particle size and particle porosity were 1294 g L^{-1}, 1012 g L^{-1}, 483 μm and 0.73 mL_{pores} $mL^{-1}_{particle}$, respectively.

Batch equilibrium isotherms for three different temperatures 283/288, 298 and 333 K were found for vanillin and syringaldehyde in aqueous solutions. Experimental results were fitted to Langmuir and Freundlich isotherm models. Equilibrium isotherms were validated by fixed bed studies at different temperatures and feed concentrations. A mathematical model comprising the equilibrium isotherms, linear driving force approximation, and intraparticle mass transfer resistances was used to describe the adsorption/desorption histories of concentration at the outlet of the fixed bed experiments. Although Langmuir model reasonably fit to the experimental results, the empirical Freundlich model was best to describe the experimental results for equilibrium concentrations bellow 1 g L^{-1}.

* Corresponding author.
E-mail address: arodrig@fe.up.pt (A.E. Rodrigues).

http://dx.doi.org/10.1016/j.cej.2015.12.041
1385-8947/

Nomenclature

A	cross sectional area of the bed (m^2)
C_e	equilibrium concentration of the adsorbate in the bulk solution ($g\ L^{-1}$)
C_{feed}	initial feed concentration ($g\ L^{-1}$)
C_0	solute concentration at column inlet ($g\ L^{-1}$)
C	solute concentration at column outlet for time t ($g\ L^{-1}$)
C_i	concentration in the bulk fluid phase for the species i ($g\ L^{-1}$)
D_{ax}	axial dispersion coefficient ($m^2\ min^{-1}$)
$D_{pe,i}$	effective pore diffusivity ($m^2\ min^{-1}$)
$D_{m,i}$	molecular diffusivity ($m^2\ min^{-1}$)
f_h	dry particle to wet particle mass ratio ($g_{dry\_resin}\ g^{-1}_{wet\_resin}$)
$\Delta H_{isosteric}$	isosteric adsorption enthalpy ($kJ\ mol^{-1}$)
K_L	constant related to the free energy of adsorption for Langmuir isotherm ($L\ g^{-1}$)
K_F	constant indicative of the relative capacity of the adsorbent for Freundlich isotherm ($(g\ g^{-1}_{dry\_resin})\ (L\ g^{-1})^{1/n}$)
k_{LDF}	linear driving force kinetic rate constant (min^{-1})
L_b	bed length (m)
Pe	Peclet number (dimensionless)
q_e	amount of solute adsorbed per dry weight unit of adsorbent at equilibrium ($g\ g^{-1}_{dry\_resin}$)
q_m	maximum adsorption capacity for Langmuir isotherm ($g\ g^{-1}_{dry\_resin}$)
q_0	amount of solute adsorbed in equilibrium with C_0 ($g\ g^{-1}_{dry\_resin}$)
q_{ads}	adsorbed amount ($g\ g^{-1}_{dry\_resin}$)
$q_{ads,exp}$	experimental adsorbed amount ($g\ g^{-1}_{dry\_resin}$)
$q_{ads,theor}$	theoretical adsorbed amount ($g\ g^{-1}_{dry\_resin}$)
q_{des}	desorbed amount ($g\ g^{-1}_{dry\_resin}$)
$\frac{dq_i^*}{dC_i}$	slope of the adsorption equilibrium isotherm
q_i	average adsorbed phase concentration of species 'i' in the adsorbent particles ($g\ g^{-1}_{dry\_resin}$)
q_i^*	adsorbed phase concentration in equilibrium with the bulk concentration at time t and position z ($g\ g^{-1}_{dry\_resin}$)
Q	flow rate ($m^3\ min^{-1}$)
R	ideal gas constant ($kJ\ mol^{-1}\ K^{-1}$)
r_p	radius of the adsorbent particle (m)
t	time (min)
T	absolute temperature (K)
$t_{st,exp}$	experimental stoichiometric time (min)
$t_{st,theor}$	theoretical stoichiometric time (min)
u_i	interstitial velocity ($m\ min^{-1}$)
V_p	volume of pores ($L_{pores}\ g^{-1}_{dry\_resin}$)
V_b	bed volume (m^3)
$V_{m,i}$	molar volume of solute at its normal boiling point ($cm^3\ mol^{-1}$)
z	axial position (m)

Greek letters

ε_P	particle porosity ($L_{pores}\ L^{-1}_{particle}$)
ε_b	bed porosity
μ	viscosity of the solution (cP)
ρ_S	solid density ($g_{dry\_resin}\ L^{-1}_{dry\_resin}$)
ρ_{app}	particle apparent density ($g_{wet\_resin}\ L^{-1}_{wet\_resin}$)
τ	tortuosity factor (dimensionless)
ϕ	association factor of the solvent (dimensionless)
Ω	linear driving force factor (dimensionless)

Abbreviations

LDF	linear driving force
pKa	acid dissociation constant

1. Introduction

Nowadays, industries worldwide are developing new strategies towards environmental and economic sustainable processes to provide efficient biomass conversion into bio-based chemicals, platform chemicals, fuels and energy [1].

Lignin is one of the most important components of side-streams from lignocellulosic-based biorefineries and pulp and paper industries and it has been considered for valorization due to its chemistry and properties. The oxidation of lignin at controlled conditions is one of the possible valorization routes, producing vanillin and syringaldehyde [2,3], among other compounds [4].

Vanillin and syringaldehyde are two phenolic aldehydes of great importance since they can be used as ingredients by flavor and fragrance industry [5–7] and as precursors of synthesis of several second-generation fine chemicals [8] such as 3,4,5-trimethoxybenzaldehyde, a building block of antibacterial agent trimethoprim [9] or levodopa, used for Parkinson's disease treatment [8]. Vanillin has the additional potential of being used as food preservative due to its antioxidant and antimicrobial properties [10,11]. Currently, 85% of vanillin world supply is synthesized from oil derived guaiacol and the remaining 15% come from lignin originated from softwoods [12], although an increase of vanillin produced from ferulic acid has also been reported [13]. Table S1 (Supplementary Material) summarizes the main physical and chemical properties of these aldehydes.

Several separation and purification sequences to obtain purified fractions of vanillin and syringaldehyde from oxidized lignin media, where a stage of solid–liquid adsorption is frequently included, have already been suggested and summarized elsewhere [14].

The majority of adsorption studies performed report the recovery of functionalized phenolic monomers from oxidized lignin medium by ion exchange resins being particularly focused on vanillin [15–17]. The application of zeolites has also been evaluated by Derouane and Powell [18].

To our knowledge adsorption studies conducted for monocomponent aqueous solutions of syringaldehyde are inexistent. There is only one study in literature reporting the recovery of syringaldehyde from an oxygen delignification spent liquor with a polymeric resin [19].

Main studies with aqueous model vanillin solutions assessed the potential of ionic resins [20,21]. Recently, the application of polymeric resins to recover vanillin gained considerable interest [19,22–27] for many reasons: adsorption of phenolics onto nonpolar resins is feasible due to the existence of both hydrophobic and hydrophilic groups in the molecule; the pH is maintained constant along the process avoiding precipitation; these resins are chemically stable and inert being suitable for applications under a wide variety of conditions; phenolics recovery and resin regeneration can be performed simultaneously in one step; and their adsorptive properties can be modelled by the surface hydrophobicity, surface area and porosity [28]. The acid dissociation constant pKa of the adsorbate also determines the adsorption capacity [29]. The highest adsorption is achieved for the neutral form of the compounds, assured by a pH value of the solution higher than its pKa.

Phenolic compounds adsorption onto nonpolar resins is commonly explained by the occurrence of weak physical interactions mainly of the van der Waals forces type (e.g. permanent dipole-induced dipole or induced dipole-induced dipole) [29–31]. Since the phenolic compounds have hydrogen donors, some authors

have studied the effect of functional groups (e.g. phenolic hydroxyl or carbonyl, acetyl, amine or methoxy groups) in polymeric resins as promoters of hydrogen bonding to improve the adsorption capacity for these compounds [32–36].

In the present work vanillin and syringaldehyde adsorption and desorption studies were performed employing the polymeric adsorbent Sepabeads SP700, known for having a large surface area and great adsorptive capabilities. Initially, the adsorbent was characterized regarding solid density, apparent density, particle size and moisture content. Afterwards, batch adsorption studies of vanillin and syringaldehyde in aqueous solution were assessed for different temperatures, obtaining the respective equilibrium isotherms. Fixed bed studies for different feed concentrations and temperatures were performed to validate the isotherm equations obtained. A mathematical model to describe the concentration profile with time was developed.

2. Experimental description

2.1. Chemicals and adsorbents

Typical phenolic compounds resulting from hardwood lignin oxidation, vanillin and syringaldehyde, were studied. Their physical and chemical characteristics are shown in Table S1 (Supplementary Material). Model solutions of vanillin (Sigma, purity ⩾ 98%) and syringaldehyde (Sigma Aldrich, purity ⩾ 98%) were prepared in deionized water and filtered through a 0.2 μm nylon membrane (whatman®).

The adsorption and desorption experiments were performed with a styrene–divinylbenzene-based synthetic adsorbent Sepabeads SP700 (Mitsubishi Chemical Corporation). Deionized water and 0.1 M $NaHCO_3$ (BDH Laboratories) were used in fixed bed studies and column regeneration, respectively. The adsorbent was washed prior to use with several solutions encompassing deionized water, methanol (Merck), methanol acidified with 0.1% formic acid (Chem-Lab).

2.2. Physical and chemical characterization of the adsorbent

Sepabeads SP700 resin was characterized concerning particle size, solid density, apparent density, particle porosity and water content. After being cleaned and prepared as described in 2.4, moisture content was assessed by weighting a known amount of resin before and after drying it at 105 °C. A dry to wet resin volume ratio was assessed by measuring the volume occupied by a certain amount of resin before and after drying at 105 °C. This analysis allowed converting the apparent density and volume of pores into wet volume of resin and comparing the experimental values with the values given by supplier.

Particle size distribution was determined by laser dispersion using a particle size analyzer (Coulter, LS230) and samples were used in wet form.

Helium pycnometry analysis was performed with previously dried resin at 105 °C to obtain the solid (or skeletal) density. This analysis measures the change in pressure of a certain amount of compressed helium gas filling a reference chamber with a known volume expanding into a second chamber containing the material to be analyzed. Helium readily diffuses into small pores, accessing larger pores than its atomic diameter of 3 Å [37].

In opposition to helium gas that readily penetrates into very fine pores, mercury is a non-wetting liquid that does not penetrate pores under atmospheric pressure. Thus, an external pressure must be applied in order to force the mercury to enter in a pore. Taking into account these principles, apparent density and volume pore size distribution can be assessed. A Quantachrome PoreMaster apparatus (Boynton Beach, FL, USA) at 20 °C was used in the analysis. It was assumed mercury density, surface tension and contact angle of 13.579 g mL^{-1}, 480 erg cm^{-2} and 140°, respectively. The porosimetry analysis was performed from 20 psi to 59,000 psi and covered pore diameters in the range of 3.6 nm and 10.6 μm. Samples were previously dried at 105 °C. It was used penetrometers of 50 g in mercury weight and about 0.4 g (dried weight) of sample.

Particle porosity and volume of pores were estimated by the following expressions:

$$\rho_{app} = \frac{1}{0.348}(1 - \varepsilon_P)\rho_S \quad (1)$$

$$V_P = \frac{1}{0.348\rho_{app}} - \frac{1}{\rho_S} \quad (2)$$

where ρ_S ($g_{dry\_resin}\ L^{-1}_{dry\_resin}$) is the solid density, ρ_{app} ($g_{wet\_resin}\ L^{-1}_{wet\_resin}$) is the particle apparent density, ε_P ($L_{pores}\ L^{-1}_{particle}$) is the particle porosity and V_p ($L_{pores}\ g^{-1}_{dry\_resin}$) is the volume of pores. 0.348 $g_{dry\_resin}\ L_{wet\_resin}\ g^{-1}_{wet\_resin}\ L^{-1}_{dry\_resin}$ is the factor to convert apparent density from $g_{dry\_resin}\ L^{-1}_{dry\_resin}$ to $g_{wet\_resin}\ L^{-1}_{wet\_resin}$.

2.3. Analytical method (HPLC-UV)

The phenolics concentration was determined by high performance liquid chromatography with ultraviolet detection (HPLC-UV). A Knauer HPLC system equipped with a Smartline 5000 online degasser, a Smartline 1000 quaternary pump, and a 2600 UV – DAD was used. The analytical column was an ACE 5 C18-pentafluorophenyl group (250 × 3.0 mm, 5 μm) with a guard column of the same material. The detection length was set to 280 nm and the volume of injection loop was 20 μL. Standard solutions and samples were filtered before injection using a 0.2 μm syringe filter (VWR). Chromatograms were run at room temperature and 0.4 mL min^{-1} at isocratic elution. The eluent was composed by methanol:water (50%:50% V/V) acidified with formic acid (0.1% V/V) previously filtered through a 0.20 μm pore size nylon filter (Whatman).

2.4. Initial resin preparation and cleaning

The resin was initially handled to remove any contaminant or monomers before batch and fixed bed experiments. Thus, the resin was brought into contact with a set of different solutions, in batch mode, using a ratio of 3 bed volumes, at room temperature. Initially, the resin was rinsed with deionized water and placed with fresh deionized water in an orbital shaker (IKA®HS 260) at 160 rpm for about 0.5 h. This step was repeated one more time. The resin was then rinsed with methanol and placed in an orbital shaker at 160 rpm with methanol for about 0.5 h. The methanol was replaced by acidified methanol (0.1% formic acid) and shaken at 160 rpm for 0.5 h. Afterwards, the resin was rinsed with water and acidified water (0.1% formic acid) was added. The mixture was agitated for 0.5 h and this step was repeated twice using deionized water.

2.5. Batch adsorption studies

Mono-component batch experiments for vanillin and syringaldehyde were conducted with 0.04 L of 4 g L^{-1} and 6 g L^{-1} solutions of each compound. Different amounts of adsorbent were used, ranging from 0.1 to 0.5 g of dry weight. Batch samples were shaken in a thermostatic water bath shaker (GLF model 3018, Germany) for 72 h at the desired temperature, in order to ensure that the equilibrium was met. Equilibrium adsorption onto each

adsorbent was performed for three different temperatures 283/288 K, 298 K and 313 K employing the batch bottle point method.

Each sample was immediately filtered through a syringe filter with 0.2 μm. The initial feed concentration and equilibrium concentrations of adsorption were quantified by HPLC-UV. pH was monitored and no significant change was observed during the adsorption experiments (around 4.5–4.9 for vanillin and 5.7–6.2 for syringaldehyde).

The adsorption capacity of the adsorbent for a specific solute corresponds to the adsorbed amount reached in a saturated solution. In batch systems, the amount of solute that disappears from the solution is adsorbed onto the adsorbent. Thus, adsorption capacity can be easily accessed through a material balance in the following way:

$$q_e = \frac{(C_{\text{feed}} - C_e)V}{W} \tag{3}$$

where q_e (g $g^{-1}_{\text{dry\_resin}}$) is the adsorption capacity at equilibrium, C_{feed} (g L^{-1}) is the initial concentration of solute in the solution, C_e is the equilibrium concentration of solute in the solution (g L^{-1}), V (L) is the initial volume solution and W (g) is the weight of dry resin.

2.6. Fixed bed adsorption studies

Fixed bed adsorption studies onto Sepabeads SP700 were carried out in a jacketed glass column (Götec, Germany) of 5.6 cm length and 1 cm internal diameter. Bed porosity (ε_b) of 0.35 and Peclet number (Pe) of 98 were estimated by tracer experiments using blue dextran. Aqueous vanillin or syringaldehyde solutions were pumped into the column with a Smartline Pump 1000 (Knauer, Germany) and isothermal conditions were assured with a thermostatic water bath (Lauda). Experiments were performed for different temperatures (298 and 313 K) and feed concentrations (0.4, 1 and 4 g L^{-1}) at fixed flow rate (approx. 5 mL min^{-1}).

The column was fed with the solution at fixed or constant temperature and samples were collected at the column outlet, diluted and quantified by HPLC-UV as described in 2.3.

The experimental stoichiometric time ($t_{\text{st,exp}}$, min) was determined by the following expression [38], for constant feed flow

$$t_{\text{st,exp}} = \int_0^{\infty} \left(1 - \frac{C}{C_0}\right) dt \tag{4}$$

where C_0 (g L^{-1}) is the concentration of solute at column inlet, C (g L^{-1}) is the solute concentration at column outlet for time t (min). The $t_{\text{st,exp}}$ can be calculated by the area underneath the plot $1 - C/C_0$ vs time. The integral was estimated applying the trapezoidal rule.

The experimental stoichiometric time was compared with the theoretical one ($t_{\text{st,theor}}$, min) estimated with the equilibrium isotherm model obtained (Langmuir or Freundlich) as following [39]:

$$t_{\text{st,theor}} = \frac{L_b}{u_i}\left[1 + \left(\frac{1-\varepsilon_b}{\varepsilon_b}\right)\left(\frac{q_0 \rho_{\text{app}} f_h}{C_0}\right)\right] \tag{5}$$

where q_0 (g $L^{-1}_{\text{wet\_adsorbent}}$) is the amount of solute adsorbed in equilibrium with C_0, ρ_{app} ($g_{\text{wet\_resin}}$ $L^{-1}_{\text{wet\_resin}}$) is the apparent density and f_h ($g_{\text{dry\_resin}}$ $g^{-1}_{\text{wet\_resin}}$) is the dry particle to wet particle mass ratio, ε_b is the bed porosity, L_b (m) is the bed length and u_i (m min^{-1}) is the interstitial velocity.

The interstitial velocity was calculated as [40]:

$$u_i = \frac{Q}{A\varepsilon_b} \tag{6}$$

where Q (m^3 min^{-1}) is the flow rate and A (m^2) is the cross sectional area of the bed.

The experimental adsorbed amount of vanillin and syringaldehyde ($q_{\text{ads,exp}}$, g $g^{-1}_{\text{dry\_resin}}$), was calculated with the following expression

$$q_{\text{ads,exp}} = \frac{QC_0 t_{\text{st,exp}}}{V_b(1-\varepsilon_b)\rho_{\text{app}} f_h} - \frac{\varepsilon_b C_0}{(1-\varepsilon_b)\rho_{\text{app}} f_h} \tag{7}$$

where V_b (m^3) is the bed volume.

Two desorption studies (one for each solute and feed concentration of approximately 1 g L^{-1}) were performed and concentration profiles were quantified as described in 2.3. The experimental amount desorbed (q_{des}, g $g^{-1}_{\text{dry\_resin}}$) was calculated with the following Eq. (8):

$$q_{\text{des}} = \frac{\int_0^t QCdt}{V_b(1-\varepsilon_b)\rho_{\text{app}} f_h} - \frac{\varepsilon_b C_0}{(1-\varepsilon_b)\rho_{\text{app}} f_h} \tag{8}$$

The removal percentage for each adsorption and desorption cycle was estimated considering the ratio between estimated $q_{\text{ads,exp}}$ and q_{des}.

After each run, the column was regenerated by eluting about 17 bed volumes of a 0.1 M $NaHCO_3$ solution and rinsing with deionized water until reaching the initial water pH of 5.5–6 (about 400 bed volumes), thus, assuring the removal of any residual vanillin or syringaldehyde.

3. Mathematical modelling

3.1. Adsorption equilibrium modelling

Langmuir and Freundlich models were studied to describe the adsorption equilibrium data obtained for vanillin and syringaldehyde in aqueous solution onto Sepabeads SP700 resin.

The Langmuir isotherm [41] defines monolayer adsorption onto homogeneous surface containing a finite number of adsorption sites of uniform energy with no interaction occurring among the adjacent adsorbed molecules. The adsorption is considered reversible and the maximum adsorption corresponds to the saturation of the monolayer of molecules adsorbed on the adsorbent surface. Graphically it is observed a plateau which corresponds to an equilibrium saturation point where no further adsorption takes place once the sites are occupied with the adsorbates. It can be described by the following Eq. (9), considering liquid–solid adsorption:

$$q_e = \frac{q_m K_L C_e}{1 + K_L C_e} \tag{9}$$

where q_m (g $g^{-1}_{\text{dry\_resin}}$) is the maximum adsorption capacity and K_L (L g^{-1}) is the constant related to the free energy of adsorption.

The Freundlich isotherm [42] is an empirical equation that describes the adsorption process on heterogeneous surfaces. This model assumes the existence of different adsorption energies grouped into patches of the same magnitude, which are independent and do not interact with each other [43]. The formation of the different patches of adsorbed molecules in the Freundlich model can be expressed by the following equation:

$$q_e = K_F C_e^{1/n} \tag{10}$$

where K_F ((g $g^{-1}_{\text{dry\_resin}}$) (L g^{-1})$^{1/n}$) is the constant indicative of the relative capacity of the adsorbent and n is the Freundlich exponent (dimensionless). When n is higher than 1 it indicates a favorable adsorption. K_F and n are empirical constants that indicate the curvature and steepness of the isotherm.

Freundlich model is commonly used to explain the adsorption of organic compounds from aqueous streams onto activated carbon [43].

Each isotherm parameters were determined by least-squares fitting of the data through minimizing the sum of the squared

residuals between the experimental data points and the estimated values obtained by the model.

The isosteric heats of adsorption, $\Delta H_{isosteric}$ (kJ mol^{-1}), for vanillin and syringaldehyde aqueous solution were calculated from the equilibrium data obtained at different temperatures with the derived Clausius–Clapeyron equation [44,45]:

$$\frac{\partial(\ln C_e)}{\partial(\frac{1}{T})} = \frac{\Delta H_{isosteric}}{R} \tag{11}$$

where C_e (g L^{-1}) is the equilibrium concentration of vanillin or syringaldehyde given by each model for a constant loading amount, R (kJ mol^{-1} K^{-1}) is the ideal gas constant, T (K) is the absolute temperature. This equation is derived from the Gibbs–Helmholtz equation at temperature T considering that: (1) at equilibrium, the chemical potentials of the solute in the bulk liquid and adsorbent phases are equal; (2) the activity of the solute on the adsorbent phase remains constant with temperature change if the amount adsorbed is kept constant and (3) the solution exhibits an ideal behavior and thus, the activity of the solute is equal to the concentration of solute in the bulk liquid phase, valid for dilute solute concentration in the mobile phase [45].

Considering that $\Delta H_{isosteric}$ is independent of the temperature, it corresponds to the slope of the plot of the isostere ln Ce vs $1/T$ for different loading amounts (q_e).

3.2. Fixed bed modelling

The axial dispersed plug flow model was used to fit the experimental breakthrough curves obtained for each of the studied phenolics. The mathematical model applied assumes isothermal adsorption, plug flow with axial dispersion, constant bed voidage and no radial gradients within the bed. Effective mass transfer between the fluid and the solid is described by the linear driving force (LDF) model [46].

The mathematical model encompasses a set of algebraic and differential equations that includes the mass balance for the liquid phase, the equilibrium isotherm between the fluid and the solid phases, and the mass transfer between the liquid and solid phases.

The mass balance equation of species 'i' in the liquid phase in a bed volume element is defined by the following equation:

$$D_{ax}\frac{\partial^2 C_i(z,t)}{\partial z^2} - u_i\frac{\partial C_i(z,t)}{\partial z} - \frac{\partial C_i(z,t)}{\partial t} - \left(\frac{1-\varepsilon_b}{\varepsilon_b}\right) f_h\, \rho_{app}\frac{\partial q_i(z,t)}{\partial t} = 0 \tag{12}$$

D_{ax} (m^2 min^{-1}) is the axial dispersion coefficient, C_i (g L^{-1}) is the concentration in the bulk fluid phase for the species i, u_i is the interstitial velocity (m min^{-1}), q_i (g $g^{-1}_{dry\_resin}$) is the average adsorbed phase concentration of species 'i' in the adsorbent particles, z (m) and t (min) are the axial position and time variables, respectively, and 'i' concerns the solute studied (e.g. vanillin or syringaldehyde).

The Danckwerts boundary conditions were applied to define the boundary conditions of the mass balance equation:

$$\begin{cases} z = 0 \rightarrow D_{ax}\frac{\partial C(z,t)}{\partial z}\Big|_{z=0} = u_i[C(0,t) - C_0] & (13) \\ z = L \rightarrow \frac{\partial C(z,t)}{\partial z}\Big|_{z=L} = 0 & (14) \end{cases}$$

The following initial conditions, of a clean bed, were considered:

$$\begin{cases} C(z,0) = 0 & (15) \\ q(z,0) = 0 & (16) \end{cases}$$

The LDF model was applied to estimate the contribution of mass transfer resistances. This expression is obtained considering a parabolic concentration profile within a spherical particle and it indicates that the rate of adsorption is proportional to the driving force (difference between adsorbed phase concentration in equilibrium with the bulk fluid concentration and the average adsorbed phase concentration in the particle) still required to reach equilibrium:

$$\frac{\partial q_i(z,t)}{\partial t} = k_{LDF}[q_i^*(z,t) - q_i(z,t)] \tag{17}$$

where, q_i^* (g $g^{-1}_{dry\_resin}$) is the adsorbed phase concentration in equilibrium with the bulk concentration at a certain time and position and k_{LDF} (min^{-1}) is the LDF kinetic rate constant.

k_{LDF} was estimated by Eq. (18) and considers homogeneous particle [47]:

$$k_{LDF} = \frac{\Omega D_{pe,i}}{f_h \rho_{app} r_p^2 \frac{dq_i^*}{dC}} \tag{18}$$

where r_p (m) is the radius of the adsorbent particle, $D_{pe,i}$ (m^2 min^{-1}) is the effective pore diffusivity, Ω (dimensionless) is the LDF factor equal to 15 considering spherical particles, $\frac{dq_i^*}{dC_i}$ is the slope of the adsorption equilibrium isotherm and q_i^* (g $g^{-1}_{dry\_resin}$) is the adsorbed phase concentration in equilibrium with the bulk concentration at time t in the position z. In the same way as Žabková et al. [22], mass transfer coefficients were calculated using the slope of the chord ($\Delta q/\Delta C$).

The axial dispersion in the packed bed was estimated by the following expression, using the experimental Peclet number obtained [40]

$$Pe = \frac{u_i L_b}{D_{ax}} \tag{19}$$

The effective pore diffusivity $D_{pe,i}$ (m^2 min^{-1}) was calculated by the following expression [48]:

$$D_{pe,i} = \frac{\varepsilon_p D_{m,i}}{\tau} \tag{20}$$

where $D_{m,i}$ (m^2 min^{-1}) is the molecular diffusivity of solute 'i' in the solvent and τ is the tortuosity factor (estimated by the Wakao and Smith model [49], corresponding to the inverse of the particle porosity).

$D_{m,i}$ was estimated for each solute by the Wilke–Chang correlation [48,50]:

$$D_{m,i} = 4.44 \times 10^{-10}\frac{T\sqrt{\phi M}}{\mu V_{m,i}^{0.6}} \tag{21}$$

where ϕ is the association factor of the solvent, which accounts for solute–solvent interactions (Wilke and Chang [50] suggest an association factor of 2.6 when the solvent used is water), M (g mol^{-1}) is the molecular weight of the solvent, μ (cP) is the viscosity of the solvent, $V_{m,i}$ (cm^3 mol^{-1}) is the molar volume of solute at its normal boiling point estimated by the simple additive method proposed by Partington [51].

The model Eqs. (12)–(16) were solved numerically with gPROMS (General Process Modelling System, version 3.7.1) using one of its integrated solvers, DASOLV, and discretizing the axial domain using orthogonal colocation method on finite elements over 100 elements with second order polynomials in each element. The mathematical model contains a system of partial differential and algebraic equations (PDAEs).

Table 1
Physical chemical properties of the resin Sepabeads SP700 given by the supplier, experimentally obtained and found in literature.

	Suppliers information	This work	Reported in literature [52]
Matrix	Styrene–Divinylbenzene	–	–
Apparent density of wet adsorbent ($g\,L^{-1}$)	1010	1012	–
Moisture content%	60–70	68.2	–
Pore volume ($mL\,g^{-1}$)	2.3	2.07	2.05
Average porosity of the particle	0.81	0.73	–
Average particle size (μm)	450	483	–
Specific surface area ($m^2\,g^{-1}$)	1200	–	1160
Average pore radius (Å)	90	–	35

4. Results and discussion

4.1. Physical and chemical characterization of the resins

Sepabeads SP700 resin (batch number 2A507) was characterized as described in Section 2.2.

In general, the values found in this work for the physical and chemical properties of the adsorbent were similar to those reported in literature and given by the supplier, as summarized in Table 1.

Moisture determination was repeated 6 times and the average value obtained for Sepabeads SP700 resin was 68.2% (±0.5%). A volume ratio of dry to wet resin of 0.92 $mL_{dry}\,mL_{wet}^{-1}$ was obtained.

Helium volume was measured in triplicate and the solid (or skeletal) density obtained was 1294 (±1) $g_{dry\_resin}\,L_{dry\_resin}^{-1}$.

In the mercury intrusion porosimetry analysis, the apparent density is obtained by the difference between the volume of mercury needed to fill a penetrometer before and after placing a known amount of sample. At atmospheric pressure, the mercury will resist entering in the pores with a diameter lower than 6 μm

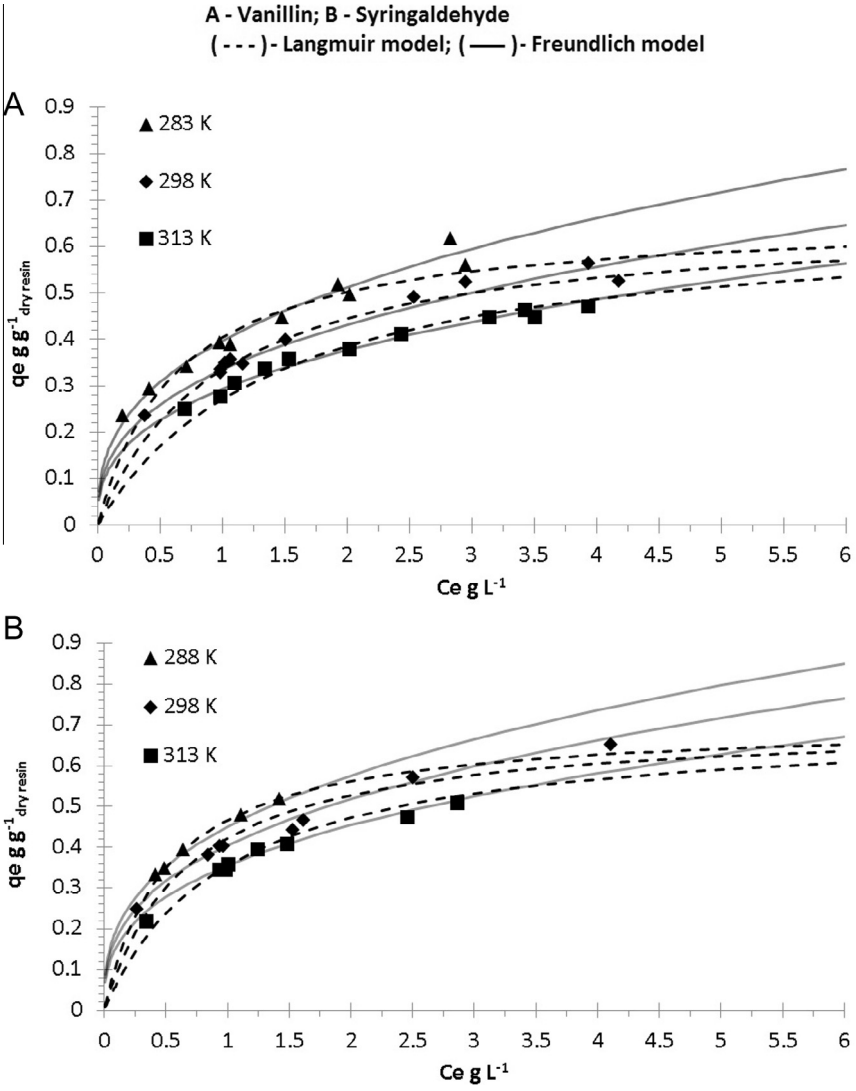

Fig. 1. Adsorption isotherms of vanillin (A) and syringaldehyde (B) in water onto the adsorbent Sepabeads SP700 at different temperatures. The dots represent experimental data, the lines (—) the Freundlich model plots and the dashed lines (- -) the Langmuir model plots.

[53]. Since the pressure used in this step is slightly higher (2.5 atm/36.7 psi), some macropores might have been intruded by the mercury and thus, the apparent density may be overestimated. Nonetheless, a similar value of apparent density to the one given by the supplier was obtained (Table 1).

The mercury intrusion porosimetry also evaluates the volume pore size distribution of macropores and mesopores (covering pore diameters in the range of 3.6 nm and 10.6 μm) and particle porosity. About 69.5% of all the intruded volume corresponded to macropores, considering that all diameters above 0.05 μm are macropores [38] and the remaining volume of 30.5% corresponded to mesopores (assuming that mesopores diameters are between 0.05 μm and 0.002 μm) [38]. This led to conclude that macropores are predominant in the resin. Additionally, it is important to refer that the resin particles might contain pores inferior to 3.6 nm and thus some mesopores and micropores were not quantified by the mercury porosimetry analysis. This last assumption is supported by Li et al. [52] which stated that Sepabeads SP700 resin has a low proportion of micropores (<2 nm). The volume of pores found in this work (2.07 mL $g^{-1}_{dry\_resin}$) was slightly lower than the one estimated through Eq. (2) with values reported by the supplier (Table 1). The corresponding particle porosity obtained was of 0.73 $L_{pores}\ g^{-1}_{dry\_resin}$ (Table 1).

Specific surface area given by the supplier is consistent with that obtained by Li et al. [52] (Multipoint BET method). However, the authors reported a predominant average pore radius of 35 Å, more than one-half lower than the value given by supplier (Table 1).

Table 2
Equilibrium parameters obtained for adsorption of vanillin and syringaldehyde onto Sepabeads SP700 resin.

Compound	Model	Parameters			
Vanillin	Langmuir	q_m	$g\ g^{-1}_{dry\_resin}$		0.663
				283 K	1.566
		K_L	$L\ g^{-1}$	298 K	1.023
				313 K	0.694
		$\Delta H_{isosteric}$	$kJ\ mol^{-1}$		−20.0
		$\sum_{i=1}^{n}(q_{exp}-q_{calc})^2$			0.0047
	Freundlich	n			2.7
				283 K	0.3977
		K_F	$(g\ g^{-1}_{dry\_resin})\ (L\ g^{-1})^{1/n}$	298 K	0.3350
				313 K	0.2927
		$\Delta H_{isosteric}$	$kJ\ mol^{-1}$		−20.5
		$\sum_{i=1}^{n}(q_{exp}-q_{calc})^2$			0.0011
Syringaldehyde	Langmuir	q_m	$g\ g^{-1}_{dry\_resin}$		0.707
				288 K	1.944
		K_L	$L\ g^{-1}$	298 K	1.476
				313 K	1.009
		$\Delta H_{isosteric}$	$kJ\ mol^{-1}$		−19.7
		$\sum_{i=1}^{n}(q_{exp}-q_{calc})^2$			0.0042
	Freundlich	n			2.8
				288 K	0.4505
		K_F	$(g\ g^{-1}_{dry\_resin})\ (L\ g^{-1})^{1/n}$	298 K	0.4076
				313 K	0.3551
		$\Delta H_{isosteric}$	$kJ\ mol^{-1}$		−20.1
		$\sum_{i=1}^{n}(q_{exp}-q_{calc})^2$			0.0028

Table 3
Mass transfer coefficients, theoretical and experimental stoichiometric times, and adsorbed amounts of vanillin and syringaldehyde for each C_0 and T, feed flow of 5 mL min^{-1} and column of 5.6 × 1 cm with 0.35 porosity.

Isotherm	Compound	C_0 g L^{-1}	T K	k_{LDF} min^{-1}	$t_{st,\ theor}$ min	$t_{st,\ exp}$ min	SD*(%)	$q_{ads,\ theor}$ g $g^{-1}_{dry\_resin}$	$q_{ads,\ exp}$ g $g^{-1}_{dry\_resin}$
Langmuir	Vanillin	0.38	298	0.043	90.5	113.5	25.41	0.182	0.235
		0.38	298	0.043	90.4	114.7	12.15	0.187	0.238
		1.02	298	0063	62.0	63.2	1.94	0.339	0.344
		1.07	298	0.064	60.4	59.4	1.66	0.346	0.343
		3.94	298	0.154	25.3	26.4	4.35	0.530	0.554
		1.11	313	0.115	48.5	52.9	9.07	0.288	0.314
Freundlich		0.38	298	0.030	114.3	113.5	0.70	0.236	0.235
		0.38	298	0.030	113.8	114.7	0.79	0.236	0.238
		1.02	298	0.058	61.8	63.2	2.27	0.338	0.344
		1.07	298	0.059	59.9	59.4	0.83	0.343	0.343
		3.94	298	0.141	26.4	26.4	0.00	0.554	0.554
		1.11	313	0.087	51.2	52.9	3.32	0.304	0.314
Langmuir	Syringaldehyde	0.96	298	0.044	80.0	79.8	0.25	0.415	0.414
		0.97	298	0.044	79.9	75.1	6.07	0.416	0.390
		4.11	298	0.128	27.7	29.2	5.42	0.607	0.641
		0.98	313	0.075	69.5	70.4	1.29	0.352	0.356
Freundlich		0.96	298	0.052	77.0	79.8	3.64	0.400	0.414
		0.97	298	0.052	76.9	75.1	2.34	0.400	0.390
		4.11	298	0.123	30.4	29.2	3.95	0.668	0.641
		0.98	313	0.077	69.7	70.4	1.00	0.352	0.356

* SD (%) corresponds to the standard deviation between the experimental and theoretical stoichiometric time, calculated with the following expression: $SD\,(\%) = \frac{|t_{st\_theor} - t_{st\_exp}|}{t_{st\_theor}} \times 100$;

Table 4
Summary of parameters used for simulation of vanillin or syringaldehyde breakthroughs, for a feed flow of 5 mL min^{-1} and a column 5.6 × 1 cm with porosity 0.35.

Compound	T K	D_{ax} m^2 min^{-1}	$D_{m,i}$ m^2 min^{-1}	$D_{pe,i}$ m^2 min^{-1}
Vanillin	298	1.04×10^{-4}	4.95×10^{-8}	2.62×10^{-8}
	313	1.04×10^{-4}	7.10×10^{-8}	3.76×10^{-8}
Syringaldehyde	298	1.04×10^{-4}	4.48×10^{-8}	2.37×10^{-8}
	313	1.04×10^{-4}	6.42×10^{-8}	3.40×10^{-8}

4.2. Adsorption equilibrium isotherms of vanillin and syringaldehyde in water onto Sepabeads SP700 resin

Equilibrium isotherms for adsorption of vanillin and syringaldehyde from aqueous solutions onto Sepabeads SP700 resin were measured and fitted to Langmuir and Freundlich models. Fig. 1 displays the experimental adsorbed amounts as a function of liquid phase concentration at equilibrium for the different temperatures and the respective fitting to Langmuir and Freundlich models. The characteristic parameters of each model are summarized in Table 2. Both models fit well to the experimental data, however, the Freundlich model describes the batch experiments better for equilibrium concentrations below 1 g L^{-1}. Several works performed with the adsorption of other phenolics onto nonpolar resins have also shown that the Freundlich model adequately describes the adsorption process [23,30,54–56].

K_L and K_F decreased with the rise of temperature, which is typical for exothermic processes. The magnitude of the temperature effect on vanillin and syringaldehyde adsorption was similar. It was observed that the equilibrium adsorption capacity for each compound studied decreased with the increase of temperature, which denotes an exothermic process, also corroborated by the estimated isosteric enthalpy value change. Published studies employing similar nonpolar resins to recover vanillin from aqueous solutions have also reported the same effect with temperature [22,23].

The isosteric enthalpy of adsorption was estimated for both models using the derived Clausius–Clapeyron relation. The isosteres ln Ce vs $1/T$ for different surface loadings are represented in Figs. S2 and S3 of Supplementary Material. The isosteric adsorption enthalpy was calculated from the slope of each isostere and was independent of surface loading. The same order of magnitude (near −20 kJ mol^{-1}) was obtained for both compounds (Table 2), indicating mainly physical adsorption onto Sepabeads SP700 resin for both compounds thus, the type of bonds involved in the adsorption phenomena are weak and the adsorption process can be reversed and resin easily regenerated [57]. These results are also in accordance with several studies performed with phenolics adsorption onto nonpolar resins, where it is commonly stated that van der Waals interaction is the main driving force for adsorption of the molecules from the bulk solution to the adsorbent phase [30,31,56].

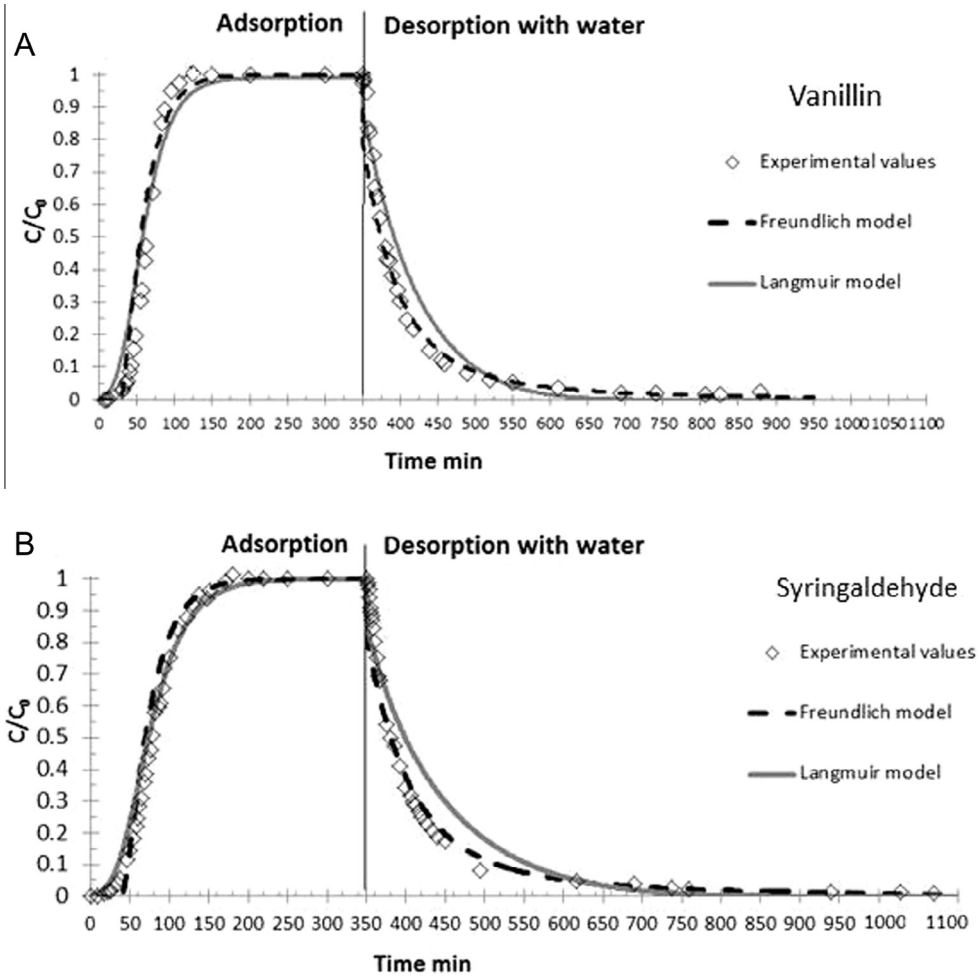

Fig. 2. Normalized concentration of vanillin (A) and syringaldehyde (B) versus time at the adsorption column outlet. Conditions: feed of 1 g L^{-1} onto the Sepabeads SP700 resin and desorption with water at 298 K, flowrate 5 mL min^{-1}, in a column of 5.6 × 1 cm and porosity 0.35: points correspond to the experimental values, the lines (—) the simulations obtained with Langmuir isotherm and the dashed lines (– –) the simulations obtained with Freundlich isotherm. The axial dispersed plug flow model with LDF approximation was used to fit the experimental breakthrough curves.

Through the plots shown in Fig. 1, it is possible to observe that resin Sepabeads SP700 adsorbs somewhat more syringaldehyde. For instance, considering an equilibrium concentration of 1 g L^{-1} of vanillin and syringaldehyde, the respective equilibrium adsorption capacities are approximately 0.335 and 0.405 g $g^{-1}_{dry\_resin}$. The maximum adsorption capacity, q_m, obtained with the Langmuir model for syringaldehyde is also slightly higher (about 7%) than the one obtained for vanillin. Being syringaldehyde the compound less soluble in water, these results are consistent with other studies [54,56,58] where it has been shown a lower adsorption for compounds showing higher solubility.

In this work, the maximum adsorption capacity of Sepabeads SP700 resin was 0.663 g $g^{-1}_{dry\_resin}$, a higher value than the ones reported in literature employing other nonpolar resins (ranging from 0.073 to 0.416 g g^{-1}). Among all, Zhang et al. [22] and Jin and Huang [26] reported the highest adsorption capacities of 0.416 g g^{-1} and 0.358 g g^{-1} for vanillin, respectively, employing synthetic cross-linked polymeric resins. Michailof et al. [23] managed to obtain maximum adsorption capacities ranging from 0.191 to 0.204 g g^{-1} using activated carbon. Žabková et al. [21] studied the nonpolar styrene divinylbenzene resin SP206, similar to the one used in this work but with lower surface area (556 m^2 g^{-1}), and reported a maximum adsorption capacity of 0.115 g $g^{-1}_{dry\_resin}$.

The Freundlich parameter n values estimated for vanillin and syringaldehyde are very similar (2.7 and 2.8, respectively) and indicative that both adsorption processes onto Sepabeads SP700 resin are favorable.

To our knowledge, there are no studies with aqueous solutions of syringaldehyde using this type of resins. Studies performed with vanillin comprise the use of activated carbon [24] and synthetic cross-linked polymeric adsorbents of hydrophobic nature [22,23,25–27]. It is important to note that published studies were performed with different methodologies and experimental conditions thus, special attention must be given when comparing final results.

4.3. Modelling of fixed bed adsorption of vanillin and syringaldehyde in water onto Sepabeads SP700 resin

Fixed bed assays with aqueous solutions of vanillin and syringaldehyde were performed in a column bed of 5.6 cm length and 1 cm of diameter for a flowrate of 5 mL min^{-1}. Different feed concentrations (0.38–4.1 g L^{-1}) and temperatures (298 and 313 K) were studied to validate the isotherm models obtained by equilibrium batch studies. The experimental conditions and results are summarized in Table 3.

The mathematical model mentioned in Section 3 was implemented to describe the breakthrough profiles obtained. The parameters of the mathematical model, axial dispersion, molecular diffusivity and effective pore diffusivity are indicated in Table 4. For each experiment carried out, the k_{LDF} estimated as described in Section 3 are specified in Table 3.

With concentration increase, the slope $\Delta q/\Delta C$ decreases resulting in higher k_{LDF} and thus, lower mass transfer resistances. Considering the experiments performed for vanillin at 298 K it is possible to observe that k_{LDF} increases linearly with the increase in concentration with a correlation coefficient R^2 of 0.9892 (Fig. S4 in Supplementary Material).

Figs. 2 and 3 show the experimental and predicted transient concentration profiles for adsorption of vanillin and syringaldehyde in aqueous solution onto Sepabeads SP700. Each breakthrough was modelled considering the equilibrium isotherms Langmuir and Freundlich obtained and the LDF approximation for the intraparticle mass transfer. The predicted behaviors demonstrate that the mathematical model considered is adequate to describe the fixed bed experiments. In general, the best breakthrough profile fitting

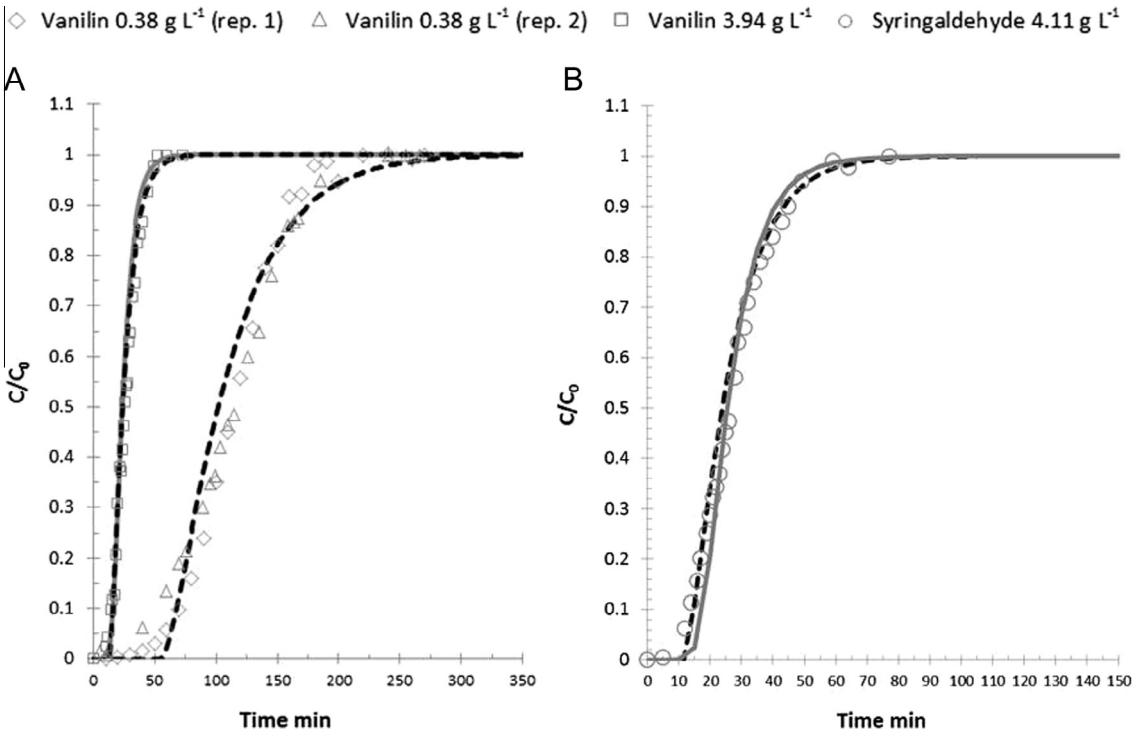

Fig. 3. Normalized concentration of vanillin (A) and syringaldehyde (B) versus time at the adsorption column outlet. Conditions: Column with Sepabeads SP700 resin for different feed concentrations at 298 K and flowrate of 5 mL min^{-1}, in a column of 5.6 × 1 cm and porosity 0.35: points correspond to the experimental points, the lines (—) to the mathematical modelling with Langmuir isotherm and the dashed lines (- -) to the mathematical modelling with Freundlich isotherm. The axial dispersed plug flow model with LDF approximation was used to fit the experimental breakthrough curves.

was achieved with the Freundlich model, particularly for the fixed bed assays performed at feed concentration of approximately 0.4 g L^{-1}. In these experiments, the stoichiometric time predicted with the Langmuir model (Table 3: 90.5 and 90.4 min for vanillin feed concentrations of 0.38 and 0.38 g L^{-1}, respectively) was significantly different than the experimental one (Table 3: 113.5 and 114.7 min). Since the equilibrium data given by Langmuir isotherm failed to describe the real situation, the breakthrough modelling represented in Fig. 3 is only shown for the Freundlich model.

In batch equilibrium adsorption experiments it was observed that the adsorption capacity was slightly higher for syringaldehyde than vanillin. This trend was also observed with fixed bed studies, for feed concentrations of 1 g L^{-1} and 4 g L^{-1}. The experimental adsorbed amounts given in Table 3 for syringaldehyde were 10–15% higher than the adsorbed amounts obtained for vanillin experiments, regardless of the selected temperature.

In the particular case of vanillin and syringaldehyde adsorption at 298 K and feed concentration of 1 g L^{-1} shown in Fig. 2, the adsorbed amount of syringaldehyde (0.390–0.414 g $g^{-1}_{dry\_resin}$, given in Table 3) was about 11% higher than that for vanillin adsorption at the same experimental conditions (0.343–0.344 g $g^{-1}_{dry\_resin}$, given in Table 3). Additionally, the experimental adsorbed amount and stoichiometric time obtained for this case satisfactorily matched the predicted values with both Langmuir and Freundlich models (Table 3).

Fig. 4 shows the experimental and model predicted breakthrough curves of the experiments performed for a feed concentration of approximately 1 g L^{-1} at 313 K. It is observed that syringaldehyde is adsorbed in a higher amount than vanillin, as also verified for the 298 K experiments. As expected, the adsorbed amount of these compounds at 313 K was smaller than at 298 K (Table 3) due to the exothermic nature of the adsorption process onto Sepabeads SP700. Previous equilibrium batch experiments showed that the adsorption capacity was negatively affected by the increase of temperature.

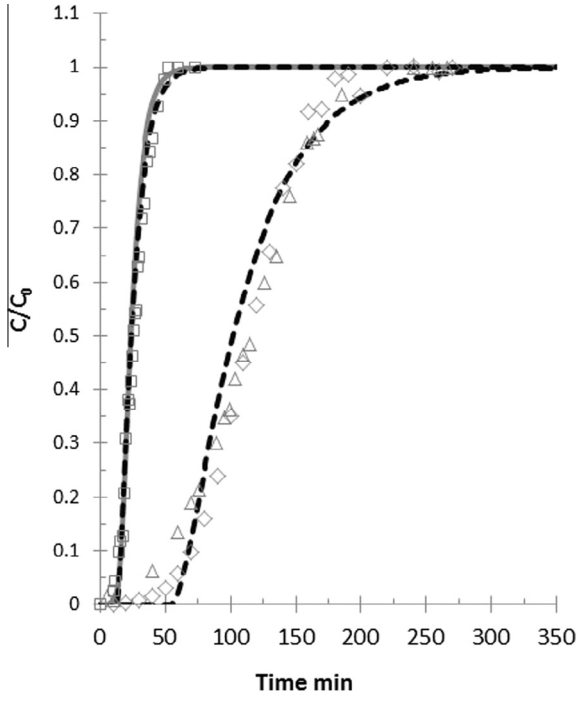

Fig. 4. Normalized concentration of vanillin and syringaldehyde versus time at the adsorption outlet. Conditions: Feed flow of 1 g L^{-1} onto the Sepabeads SP700 resin at 313 K and flowrate of 5 mL min^{-1}, in a column of 5.6 × 1 cm and porosity 0.35: Points correspond to the experimental points, the lines (—) to the mathematical modelling with Langmuir isotherm and the dashed lines (- -) to the mathematical modelling obtained with Freundlich isotherm. The axial dispersed plug flow model with LDF approximation was used to fit the experimental breakthrough curves.

Desorption studies with water were performed for the experiments with vanillin and syringaldehyde adsorption at 298 K and feed concentration of 1 g L^{-1}. After eluting 9 h with the flowrate and temperature used for adsorption, about 83–85% of the initially amount adsorbed of vanillin and syringaldehyde was desorbed. As it can be seen from Fig. 2, the shape of the desorption curve is different from the adsorption curve because of the non-linearity of the adsorption equilibrium (dispersive front). Additionally, the Freundlich model was the most suitable model describing the desorption studies performed, since the theoretical curve practically matches the experimental desorption points. The mathematical modelling using the Langmuir isotherm predicted a faster desorption rate than the one experimentally observed for both vanillin and syringaldehyde.

It is important to notice that desorption studies performed with water were considerably time-consuming and led to a high dilution of the final solution obtained. In order to obtain a more feasible desorption process other solvents must be applied when the recovery of vanillin and syringaldehyde is envisaged. Considering this, existing literature shows the advantage of employing organic solvents as eluting agent [19,59]. Wang et al. [19] demonstrated that about 95–96% of vanillin and syringaldehyde could be desorbed from the nonpolar D101 resin with 1.3 bed volumes of ethyl acetate.

5. Conclusions

Adsorption and desorption studies of vanillin and syringaldehyde onto a macroporous styrene–divinylbenzene adsorbent (Sepabeads SP700) were performed. The respective equilibrium adsorption isotherms in aqueous solutions were estimated for different temperatures. Fixed bed experiments were performed and the isotherm models were validated.

The adsorbed amounts of vanillin and syringaldehyde had a non-linear behavior with the equilibrium concentration. Equilibrium data were fitted to Langmuir and Freundlich models; however the second model was the one that better describes the experimental data. The amount of adsorbed compound decreased with the increase of temperature, thus revealing the exothermic nature of the process.

Fixed bed adsorption studies for different feed concentrations and temperatures were accomplished. The transient concentration profiles along time were well described with the axial dispersed plug flow mathematical model comprising the adsorption equilibrium isotherm and the LDF approximation to represent the intraparticle mass transfer.

Finally, desorption with water revealed to be a very time consuming process that greatly dilutes the desorbed phenolic compounds. Therefore, other studies towards improving desorption step with more efficient solvents will be conducted in order to find a more feasible desorption process for vanillin and syringaldehyde recovery.

Acknowledgements

Inês Mota gratefully acknowledges her Ph.D. scholarship (SFRH/BD/91582/2012) from Fundação para a Ciência e Tecnologia (FCT).

This work was co-financed by FCT and FEDER under Programme PT2020 (Project UID/EQU/50020/2013) and Programme COMPETE (FCOMP-01-0124-FEDER-123456).

The authors also thank to Project No. 33969 Conception of bio-based products from renewable lignocellulosic sources as precursors for bioindustry of chemical synthesis and biomaterials – funded by FEDER through the National Strategic Reference Framework.

Appendix A. Supplementary data

Supplementary data associated with this article can be found, in the online version, at http://dx.doi.org/10.1016/j.cej.2015.12.041.

References

[1] B. Kamm, M. Kamm, Principles of biorefineries, Appl. Microbiol. Biotechnol. 64 (2004) 137–145.
[2] J. Zakzeski, P.C.A. Bruijnincx, A.L. Jongerius, B.M. Weckhuysen, The catalytic valorization of lignin for the production of renewable chemicals, Chem. Rev. 110 (2010) 3552–3599.
[3] P.C.R. Pinto, E.A.B. Silva, A.E. Rodrigues, Lignin as source of fine chemicals: vanillin and syringaldehyde, in: C. Baskar, S. Baskar, R.S. Dhillon (Eds.), Biomass Conversion, Springer, Berlin Heidelberg, London, 2012, pp. 381–420.
[4] P.C.R. Pinto, C.E. Costa, A.E. Rodrigues, Oxidation of lignin from *Eucalyptus globulus* pulping liquors to produce syringaldehyde and vanillin, Ind. Eng. Chem. Res. 52 (2013) 4421–4428.
[5] M.B. Hocking, Vanillin: synthetic flavoring from spent sulfite liquor, J. Chem. Educ. 74 (1997) 1055–1059.
[6] M.N.M. Ibrahim, R.B. Sriprasanthi, S. Shamsudeen, F. Adam, S.A. Bhawani, A concise review of the natural existence, synthesis, properties, and applications of syringaldehyde, Bioresources 7 (2012) 1–23.
[7] J.E. Holladay, J.J. Bozell, J.F. White, D. Johnson, Results of Screening for Potential Candidates from Biorefinery Lignin, in Top Value-Added Chemicals from Biomass, Pacific Northwest National Laboratory and National Renewable Energy Laboratory, Richland, WA, 2007.
[8] H.-R. Bjørsvik, L. Liguori, Organic processes to pharmaceutical chemicals based on fine chemicals from lignosulfonates, Org. Process Res. Dev. 6 (2002) 279–290.
[9] Y.V. Erofeev, V.L. Afanas'eva, R.G. Glushkov, Synthetic routes to 3,4,5-trimethoxybenzaldehyde (review), Pharm. Chem. J. 24 (1990) 501–510.
[10] J. Burri, M. Graf, P. Lambelet, J. Löliger, Vanillin: more than a flavouring agent–a potent antioxidant, J. Sci. Food Agric. 48 (1989) 49–56.
[11] P.M. Davidson, A.S. Naidu, Phyto-phenols, in: A.S. Naidu (Ed.), Natural Food Antimicrobial Systems, CRC Press, Florida, 2000, pp. 265–294.
[12] L. Thiel, F. Hendricks, Study into the establishment of an aroma and fragrance fine chemicals value chain in South Africa, part three: aroma chemicals derived from petrochemical feedstocks, Tender number T79/07/03. Government Tender Bulletins. National Economic Development and Labor Council, available from: <http://www.thedti.gov.za/industrial_development/docs/fridge/Aroma_Part3.pdf> (accessed in September 2015).
[13] S.A. Solvay, retrieved from: <http://www.solvay.com/en/markets-and-products/featured-products/rhovanil-natural.html>, 2015 (accessed September 2015).
[14] I.F. Mota, P.C.R. Pinto, J.M. Loureiro, A.E. Rodrigues, Recovery of vanillin and syringaldehyde from lignin oxidation: a review of separation and purification processes, Sep. Purif. Rev., in press, http://dx.doi.org/10.1080/15422119.2015.1070178.
[15] C.D. Logan, Cyclic process for recovering vanillin and sodium values from lignosulfonic waste liquors by ion exchange, US Patent 3197359 (July 27, 1965), 1965.
[16] K.G. Forss, K.E. Fremer, E.T. Talka, Method for the isolation of vanillin from lignin in alkaline solutions, US Patent 4277626 (July 07, 1981), 1981.
[17] F. Stecker, A. Fischer, A. Kirste, A. Voitl, C.H. Wong, S. Waldvogel, C. Regenbrecht, D. Schmitt, M.F. Hartmer, Method for obtaining vanillin from aqueous basic compositions containing vanillin, WO Patent 2014006108 A1 (January 09, 2014), 2014.
[18] E.G. Derouane, R.A. Powell, Vanillin extraction process using large pore, high silica/alumina ratio zeolites, US patent 4652684 (March 24, 1987), 1987.
[19] Z. Wang, K. Chen, J. Li, Q. Wang, J. Guo, Separation of vanillin and syringaldehyde from oxygen delignification spent liquor by macroporous resin adsorption, Clean 38 (2010) 1074–1079.
[20] C. Fargues, Á. Mathias, A. Rodrigues, Kinetics of vanillin production from kraft lignin oxidation, Ind. Eng. Chem. Res. 35 (1996) 28–36.
[21] M. Žabková, E.A. Borges da Silva, A.E. Rodrigues, Recovery of vanillin from Kraft lignin oxidation by ion-exchange with neutralization, Sep. Purif. Technol. 55 (2007) 56–68.
[22] M. Žabková, M. Otero, M. Minceva, M. Zabka, A.E. Rodrigues, Separation of synthetic vanillin at different pH onto polymeric adsorbent Sepabeads SP206, Chem. Eng. Process. 45 (2006) 598–607.
[23] Q.-F. Zhang, Z.-T. Jiang, H.-J. Gao, R. Li, Recovery of vanillin from aqueous solutions using macroporous adsorption resins, Eur. Food Res. Technol. 226 (2008) 377–383.
[24] C. Michailof, G.G. Stavropoulos, C. Panayiotou, Enhanced adsorption of phenolic compounds, commonly encountered in olive mill wastewaters, on olive husk derived activated carbons, Bioresour. Technol. 99 (2008) 6400–6408.
[25] G.-Q. Xiao, X.-L. XIE, M.-C. XU, Adsorption performances for vanillin from aqueous solution by the hydrophobic-hydrophilic macroporous polydivinylbenzene/polyacrylethylenediamine IPN resin, Acta Phys.-Chim. Sin. 25 (2009) 97–102.
[26] X. Jin, J. Huang, Adsorption of vanillin by an anisole-modified hyper-cross-linked polystyrene resin from aqueous solution: equilibrium, kinetics, and dynamics, Adv. Polym. Tech. 32 (2013) E221–E230.
[27] R.A. Samah, N. Zainol, P.L. Yee, C.M. Pawing, S. Abd-Aziz, Adsorption of vanillin using macroporous resin H103, Adsorpt. Sci. Technol. 31 (2013) 599–610.
[28] B.D. Crittenden, W.J. Thomas, Adsorption Technology and Design, first ed., Butterworth and Heinemann, Oxford, 1998.
[29] R. Kunin, 1.11 Polymeric Adsorbents, in: K. Dorfner (Ed.), Ion Exchangers, De Gruyter, New York, 1991.
[30] B.C. Pan, Y. Xiong, Q. Su, A.M. Li, J.L. Chen, Q.X. Zhang, Role of amination of a polymeric adsorbent on phenol adsorption from aqueous solution, Chemosphere 51 (2003) 953–962.
[31] S. Suresh, V. Srivastava, I. Mishra, Adsorption of catechol, resorcinol, hydroquinone, and their derivatives: a review, Int. J. Energy Environ. Eng. 3 (2012) 1–19.
[32] A. Li, C. Long, Y. Sun, Q. Zhang, F. Liu, J. Chen, A new phenolic hydroxyl modified polystyrene adsorbent for the removal of phenolic compounds from their aqueous solutions, Sep. Sci. Technol. 37 (2002) 3211–3226.
[33] Z.-M. Jiang, A.-M. Li, J.-G. Cai, C. Wang, Q.-X. Zhang, Adsorption of phenolic compounds from aqueous solutions by aminated hypercrosslinked polymers, J. Environ. Sci. 19 (2007) 135–140.
[34] J. Huang, C. Yan, K. Huang, Removal of *p*-nitrophenol by a water-compatible hypercrosslinked resin functionalized with formaldehyde carbonyl groups and XAD-4 in aqueous solution: a comparative study, J. Colloid Interface Sci. 332 (2009) 60–64.
[35] J. Huang, X. Jin, S. Deng, Phenol adsorption on an N-methylacetamide-modified hypercrosslinked resin from aqueous solutions, Chem. Eng. J. 192 (2012) 192–200.
[36] J. Huang, L. Yang, X. Wu, M. Xu, Y.-N. Liu, S. Deng, Phenol adsorption on α, α′-dichloro-p-xylene (DCX) and 4,4′-bis(chloromethyl)-1,1′-biphenyl (BCMBP) modified XAD-4 resins from aqueous solutions, Chem. Eng. J. 222 (2013) 1–8.
[37] K. Asaoka, J.-Y. Bae, H.-H. Lee, Porosity of dental gypsum-bonded investments in setting and heating process, Dent. Mater. J. 31 (2012) 120–124.
[38] D.M. Ruthven, Principles of Adsorption and Adsorption Processes, John Willey and Sons, New York, 1984.
[39] A.E. Rodrigues, M.D. Levan, D. Tondeur, Adsorption: Science and Technology, first ed., Kluwer Academic Publishers, London, 1989.
[40] G. Guiochon, A. Felinger, D. Shirazi, A. Katti, Fundamentals of Preparative and Nonlinear Chromatography, second ed., Elsevier Academic Press, New York, 2006.
[41] I. Langmuir, The adsorption of gases on plane surfaces of glass, mica and platinum, J. Am. Chem. Soc. 40 (1918) 1361–1402.
[42] H.M.F. Freundlich, Kapillarchemie, Akademische Verlagsgesellschaft, Leipzig, 1909.
[43] D.D. Duong, Adsorption Analysis: Equilibria and Kinetics, Imperial College Press, London, 1998.
[44] G. Guiochon, A. Felinger, D.G.G. Shirazi, A.M. Katti, Fundamentals of Preparative and Nonlinear Chromatography, second ed., Elsevier, Oxford, 2006.
[45] S. Jacobson, S. Golshan-Shirazi, G. Guiochon, Measurement of the heats of adsorption of chiral isomers on an enantioselective stationary phase, J. Chromatogr. A 522 (1990) 23–36.
[46] E. Glueckauf, J.I. Coates, 241. Theory of chromatography. Part IV. The influence of incomplete equilibrium on the front boundary of chromatograms and on the effectiveness of separation, J. Chem. Soc. (Resumed) (1947) 1315–1321.
[47] S. Farooq, D.M. Ruthven, Heat effects in adsorption column dynamics. 2. Experimental validation of the one-dimensional model, Ind. Eng. Chem. Res. 29 (1990) 1084–1090.
[48] R.C. Reid, J.M. Prausnitz, B.E. Poling, The Properties of Gases and Liquids, fourth ed., McGraw Hill, New York, 1987.
[49] J.M. Smith, Chemical Engineering Kinetics, McGraw-Hill Chemical Engineering Series, New York, 1981.
[50] C.R. Wilke, P. Chang, Correlation of diffusion coefficients in dilute solutions, AIChE J. 1 (1955) 264–270.
[51] S. Partington, An Advanced Treatise on Physical Chemistry, Vol. I, Fundamental Principles: The Properties of Gases, first ed., Longmans, Green & Co., London, 1949.
[52] A. Li, F. Ma, X. Song, R. Yu, Dynamic adsorption of diarrhetic shellfish poisoning (DSP) toxins in passive sampling relates to pore size distribution of aromatic adsorbent, J. Chromatogr. A 1218 (2011) 1437–1442.
[53] P.A. Webb, An Introduction to the Physical Characterization of Materials by Mercury Intrusion Porosimetry with Emphasis on Reduction and Presentation of Experimental Data, Micromeritics Instrument Corp., Georgia, 2001.
[54] I. Souchon, J.A. Rojas, A. Voilley, G. Grevillot, Trapping of aromatic compounds by adsorption on hydrophobic sorbents, Sep. Sci. Technol. 31 (1996) 2473–2491.
[55] Y. Ku, K.C. Lee, Removal of phenols from aqueous solution by XAD-4 resin, J. Hazard. Mater. 80 (2000) 59–68.
[56] X.J. Wang, J.F. Zhao, S.Q. Xia, A.M. Li, L. Chen, Adsorption mechanism of phenolic compounds from aqueous solution on hypercrosslinked polymeric adsorbent, J. Envirn. Sci. 16 (2004) 919–924.
[57] G.C. Bond, Heterogeneous Catalysis: Principles and Applications, Clarendon Press, Oxford, 1974.
[58] G.F. Payne, N.N. Payne, Y. Ninomiya, M.L. Shuler, Adsorption of nonpolar solutes onto neutral polymeric sorbents, Sep. Sci. Technol. 24 (1989) 457–465.
[59] A. Li, Q. Zhang, G. Zhang, J. Chen, Z. Fei, F. Liu, Adsorption of phenolic compounds from aqueous solutions by a water-compatible hypercrosslinked polymeric adsorbent, Chemosphere 47 (2002) 981–989.